Influence of Cyclosporine A on Molecular Interactions in Lyotropic Reverse Hexagonal Liquid Crystals

Paul Ben Ishai,*,† Dima Libster,‡ Abraham Aserin,‡ Nissim Garti,‡ and Yuri Feldman†

Department of Applied Physics and Casali Institute of Applied Chemistry, The Institute of Chemistry, The Hebrew University of Jerusalem, Givat Ram Campus, Jerusalem 91904, Israel

Received: May 3, 2010; Revised Manuscript Received: July 17, 2010

We present a dielectric study of H_{II} mesophases (H_{II}) based on a GMO/tricaprylin/phosphatidylcholine/water system seeded with the peptide Cyclosporine A (CSA). The study covers a frequency range 0.01 Hz to 1 MHz and a temperature range of 293 to 319 K, with a 3 K temperature step. Three dielectric relaxation processes are observed and discussed. This picture is further elucidated by comparison with a dielectric study of the empty H_{II} mesophase system, previously published, where the same three processes were involved. A complex picture emerges whereby the CSA is intercalated between the surfactant tails yet protrudes into the interface as well. Whereas the CSA remains hydrophobic, it still influences the relaxation behavior of the GMO head and counterion movement along the interface in a nontrivial manner. The third dipolar species, the tricaprylin molecule, is also influenced by the presence of CSA. A critical temperature $T_0 = 307$ K is recognized and identified as the dehydration temperature of the surfactant heads. This induces a conformal transition in the CSA, drastically changing its effect on the three dielectric processes evident in the raw data. The implications of this behavior are discussed in detail.

Introduction

Reverse hexagonal liquid crystalline systems (H_{II}) are a class of lyotropic liquid crystals possessing an impressive potential as drug delivery systems.[1−4] They are able to entrap biologically active molecules, such as peptides and enzymes, and have been shown to be advantageous for sustained release of such agents.[2] They are characterized by densely packed, straight water-filled cylinders, exhibiting 2-D ordering. Each cylinder is surrounded by a layer of surfactant molecules that are perpendicular to the cylindrical interface such that their hydrophobic moieties point outward from the water rods. (See Figure 1.) However, the presence of a guest molecule is expected to modify the dynamic behavior of H_{II}, depending on where it is situated. An example of such is the immobilization of therapeutic peptides such as Cyclosporine A (CSA)[5,6] and desmopressin.[7] CSA is a cyclic polypeptide consisting of 11 amino acids with a molecular weight of 1202.6 g mol^{-1}. CSA has revolutionized organ transplantation and the treatment of autoimmune disorders.[8] Clinically, it has been used as one of the most effective immunosuppressive agents for transplantation medicine and also in dermatology for the treatment of inflammation and skin disorders, such as psoriasis. However, the extreme lipophilicity and high molecular weight of CSA hamper its skin penetration, leading to an accumulation in the stratum corneum and slow transport into deeper skin layers.[9] The long-term systemic administration of CSA induces harmful side effects, such as nephrotoxicity.[10] To reduce these side effects and attain greater therapeutic levels, several topical formulations have been developed. In addition to H_{II} mesophases, various routes were explored employing approaches such as emulsions, microspheres, nanoparticles, liposomes, iontophoresis, and penetration enhancers.[8]

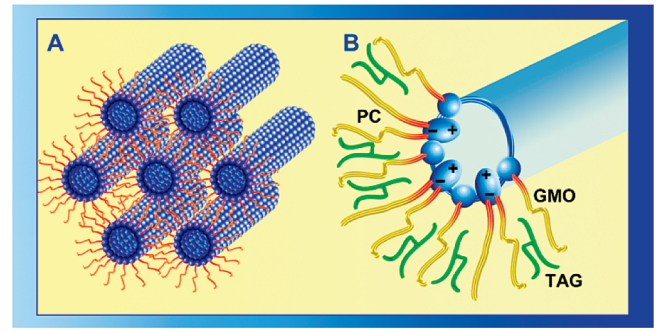

Figure 1. (A) Schematic presentation of the supramolecular organization of HII mesophase, showing the cylinder packing. (B) Schematic illustration focused on one cylinder of the mixed surfactant (GMO and PC) hexagonal system organization. Note that GMO and PC polar moieties are hydrated but that TAG is located between the lipophilic chains of the surfactants.

The physical and structural properties of H_{II} mesophases have been extensively studied by means of SAXS, ATR-FTIR, SD-NMR, DSC, and rheological techniques.[5,6,11−14] Further work into the immobilization of CSA[7] revealed its impact on the host mesophase and conformational changes within the system on a macroscopic scale and on a molecular level. However, the influence on the dynamic behavior of the H_{II} mesophase is still an open question. Some research has been carried out on the effect of incorporating CSA into monoolein/water mesophases.[15] However, in that study only at high water content and temperature was the H_{II} mesophase achieved. Consequently, the effect of additional stabilizers, such as PC and TAG, on the interface was not considered. It is of importance because the bioavailability will depend to a large extent on membrane stability and behavior, both of which will be affected by the presence of a guest molecule.

In our previous paper,[16] dielectric spectroscopy (DS) was applied as an experimental technique in the study of the empty H_{II} system. DS is particularly fruitful because of its ability to highlight relaxation dynamics over extremely wide time scales,[17]

* To whom correspondence should be addressed. Address: The Applied Physics Department, The Selim and Rachel Benin School of Computer Science and Engineering, Givat Ram Campus, The Hebrew University of Jerusalem, Jerusalem 91904, Israel. Tel: +972-2-658-5061. E-mail: paulb@vms.huji.ac.il.

† Department of Applied Physics.

‡ Casali Institute of Applied Chemistry, The Institute of Chemistry.

10.1021/jp104028m
Published on Web 09/21/2010

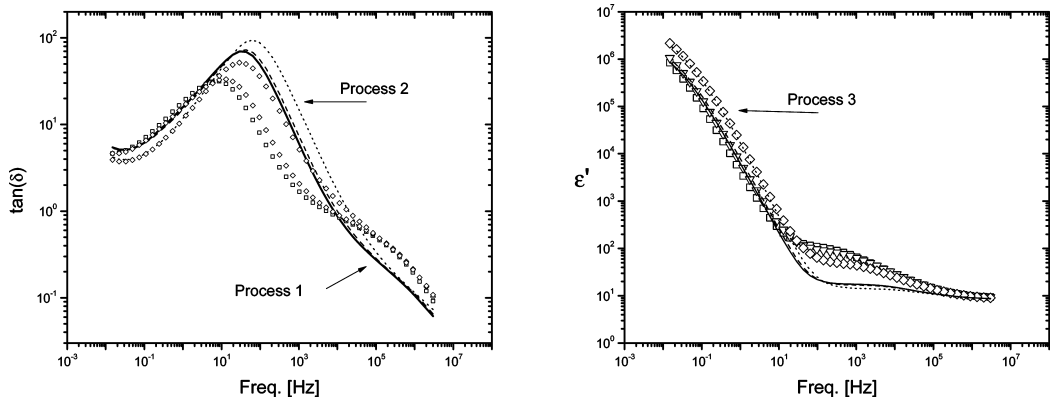

Figure 2. Tan(δ) and the real component of the dielectric permittivity, ε', of HEX_{II} mesophase with and without the drug Cyclosporine A entrapped. Three temperature slices are shown without CSA (□, 293 K; ▽, 301 K; and ◇, 319 K) and with CSA (solid line, 293 K; dashed line, 301 K; and dotted line, 319 K). Three temperature-activated processes are noted and labeled Processes 1, 2, and 3, respectively, in each. The effect due to the presence of the drug is most clearly noted in Processes 1 and 2.

especially when dealing with colloidal systems. Consequently, in our previous work, we performed a dielectric study of an H_{II} mesophase composed of GMO/tricaprylin/phosphatidylcholine/water, probing the kinetic aspects of the interface. The complex molecular behavior in and around the interfaces of the mesoscopic structures was revealed in three clearly defined dielectric relaxations. These relaxations were related to separate moieties in the interface. Of note was a critical temperature, $T_0 = 307$ K, related to the dehydration of the glycerol monooleate (GMO) headgroups. The "loosening" of the GMO headgroups accentuated the dangling motion of the phosphatidylcholine (PC) tails, evidenced by counterion motion along the PC headgroup. Furthermore, it precipitated the percolation of the large TAG molecules, intercalated in the GMO and PC tails. To exploit H_{II} as the delivery vehicle requires a close acquaintance with the relationships between the different levels of structure and dynamics of these materials.

Our purpose in this Article is to investigate just this question: How will the presence of a peptide such as CSA modify the dynamic behavior of the H_{II} mesophase, and can this change be tailored? We shall address this study from this perspective.

Materials and Methods

Monoolein, GMO (OL type, molecular weight 357 g mol^{-1}, density 0.942 gml^{-1}), distilled GMO (min. 97 wt % monoglyceride), 2.5 wt % diglyceride, and 0.4 wt % free glycerol (acid value 1.2, iodine value 68.0, melting point 37.5 °C) were obtained from Riken Vitamin (Tokyo, Japan). Tricaprylin (TAG, molecular weight 470.7 g mol^{-1}, density 0.954 gml^{-1}; 97 to 98 wt %) was purchased from Sigma Chemical (St. Louis, MO). PC (molecular weight 758 g/mol, density 1.019 gml^{-1}) of soybean origin (Epikuron 200, min. 92% PC) was purchased from Degussa (Hamburg, Germany). CSA was purchased from LC Laboratories (Woburn, MA). Water was double-distilled. All ingredients were used without further purification.

Preparation of H_{II} Mesophases. The GMO/PC/tricaprylin/water hexagonal liquid crystal with composition of 59.4 wt % GMO, 6.6 wt % tricaprylin (9:1 weight ratio), 4 wt % CSA, 10 wt % PC, and 20 wt % water was chosen for preparation of H_{II} mesophase. The sample was prepared by mixing weighed quantities of GMO, tricaprylin, and PC while heating to 80 °C. Afterward, CSA was dissolved in this mixture. An appropriate quantity of preheated water was added at the same temperature, and the samples were stirred and cooled to 25 °C. This was done in sealed tubes under a nitrogen atmosphere to avoid oxidation of the GMO and PC. The thermal stability of the peptide was verified by FTIR analysis of the Amide I band after heating and cooling cycles and DSC analysis (data not shown). The samples were allowed to equilibrate for 24 h before DS measurements.

Dielectric Measurements. Dielectric measurements on the H_{II} mesophases were carried out in a relatively narrow temperature range, $293 < T < 319$ K, with a 3 K temperature step. The narrow temperature range was chosen to concentrate on the biologically relevant aspects of the study. The frequency window was 0.01 Hz $< f <$ 1 MHz, and the measurements were made using a Novocontrol BDS 80 system (Novocontrol GmbH, Hamburg) based on an Alpha Dielectric Analyzer. The temperature control was provided by a Novocontrol Quatro Cryosystem (Novocontrol GmbH, Hamburg). The accuracy of measurement[18] in terms of tan δ is $<10^{-4}$. The samples were mounted between two gold-plated electrode plates with a diameter of 24 mm. The plates were cleaned with alcohol and dried before the samples were placed on them. Teflon spacers of 1 mm thickness were used to maintain a constant and accurately known distance between the plate electrodes.

Results

The dielectric results revealed the presence of three processes, separated by frequency and possessing differing dielectric strengths. Additionally, dc conductivity was also observed. In general, the motif established by Ben Ishai et al.[16] is maintained, but the parameters characterizing the processes are modified by the presence of CSA. For illustration, three temperature slices, with and without the presence of CSA in the mesophase, are presented in Figure 2 in terms of $\tan(\delta) = \varepsilon''/\varepsilon'$ and ε', as functions of frequency. An advantage in presenting dielectric data in terms of tan(δ) is that the relaxation peak is well-accentuated, leading to an easier determination of separate processes. This is of particular use when a relatively weak relaxation process is juxtaposed with a stronger peak. Consequently, Processes 1 and 2 are clearly separated in the tan(δ) representation. The frequency ranges for the processes were: 10^5 to 10^6 Hz for Process 1, 10 to 10^3 Hz for Process 2, and 10^{-2} to 1 Hz for Process 3. All of the processes spanned the full temperature range of the experiment. The dielectric data were fitted using an in-house fitting program, Matfit,[19] based on Matlab,[20] and a fitting function consisting of three Havrilak Negami (H−N) functions[21] with a dc conductivity term.

$$\dot{\varepsilon}(\omega) - \varepsilon_{hf} = \frac{-\sigma_{dc}}{i\omega} + \sum_{n=1}^{\delta} \frac{\Delta\varepsilon_n}{(1 + (i\omega n)^{\alpha_n})^{\beta_n}} \quad (1)$$

where σ_{dc} is the dc conductivity, ε_{hf} is the high frequency value of the dielectric permittivity,$\Delta\varepsilon_n$ is the dielectric strength, τ_n is the characteristic relaxation time for the process, and α_n and β_n range from 0 to 1. From the fitting routine, it was established that for Processes 1 and 2, β was identical to 1, leading to the so-called Cole−Cole relaxation function. As noted in Ben Ishai et al.,[16] Process 3 could only be fitted if the structural parameters of the H−N function were allowed to range between 0 and 2. The ranging of the structural parameters presents a conceptual problem. First, it rules out Maxwell−Wagner behavior, indicative of simple electrode polarization. Second, the physical interpretation of the parameters α and β with such limits is still an open debate. However, the same data when viewed in the time domain are more amenable, and their meaning is more established. This point shall be further addressed in the Discussion section.

Discussion

H−N functions are established phenomenological fits to describe frequency-based dielectric data in many complex systems.[21] The specific case $\alpha_n = 1$, $\beta_n = 1$ gives the Debye relaxation law; the case $\beta_n = 1$, $\alpha_n < 1$ corresponds to the so-called Cole−Cole (CC) equation,[22] and the case $\alpha_n = 1$, $\beta_n < 1$ corresponds to the Cole−Davidson (CD) formula.[23] The CC and CD cases can be given a microscopic interpretation.[17] In particular, the CC equation can be demonstrated as arising from an interaction of the relaxing dipole moment with its underlying physical matrix.[24] This dipole−matrix interaction provides a restrictive component to the orientational relaxation of dipole. In this regard, the broadening parameter, α, is analyzed according to a self-diffusion model describing the said interaction with the host matrix

$$\alpha = \frac{d_g}{2} \cdot \frac{\ln(\tau\omega_0)}{\ln(\tau/\tau_0)} \quad (2)$$

where d_g is the spatial fractal dimension, τ is the relaxation time, τ_0 is a scaling time providing the measure by which an interaction can be enumerated in its time interval, and ω_0 is a characteristic frequency of the diffusion of the dipole. Equation 2 relies on the relationship between the mean square distance from an arbitrary origin obtained in a time frame by the self-diffusing particle, $R^2 \propto t$, to a volume of interaction with the underlying matrix. A further derivation[25] of eq 2, based on anomalous diffusion, replaces d_g by γd_g, where γ is the anomalous diffusion exponent connecting the mean square length with the relaxation time, $R^2 \propto t^{\gamma}$. In this instance, a complete range of transport phenomena can be accounted for, including subdiffusive and superdiffusive behavior.[26]

Process 3, however, is more puzzling. Its large dielectric strength (Figure 6b, discussed below under Process 3) would initially suggest an interfacial component, yet this would be expected to conform to the usual scheme of $0 < \alpha, \beta \leq 1$. The other alternative is a transport phenomenon, recognized as the percolation of the large TAG molecule in ref 16 and confirmed by NMR measurements of TAG.[14] Consequently, Process 3 was Laplace transformed to the time domain to extract the macroscopic dipole−dipole correlation function.

$$\psi(t) = \frac{\bar{M}(t)\cdot\bar{M}(0)}{\bar{M}(0)\cdot\bar{M}(0)} = \mathcal{L}^{-1}[\dot{\varepsilon}(\omega)] \quad (3)$$

where $\bar{M}(t)$ is the macroscopic dipole moment and $\psi(t)$ is the macroscopic dipole−dipole correlation function. The power and stretched exponential function was then used to fit the data in the time domain

$$\psi(t) = At^{-\mu} \exp\left(-\left(\frac{t}{t}\right)^{\nu}\right) \quad (4)$$

where A is the amplitude of the process, τ is the characteristic relaxation time, and μ and ν are exponents ranging from 0 to 1. Equation 4 can be derived from relatively simple assumptions on the distribution of basic relaxations on a static site lattice model[27] and reflects transport processes, in particular, percolation.[17] The dielectric relaxation caused by the movement of a charge or dipole can be broken down into two components: the growth of a cooperative domain wherein the dipole is able to move, whose relaxation behavior can be characterized by a power law in its time dependence, $t^{-\mu}$, and a charge movement inside this region along a distributed set of paths, resulting in a stretched exponential behavior. This is a consequence of the less-than-ideal medium through which the transport occurs, which is characterized by a spatial fractal dimension d_g, related to the stretch exponential by the expression[17] $d_g = 3\nu$.

The results for the fitting parameters are presented in Figure 3 for Process 1, Figure 4 for Process 2 and for the dc conductivity, and in Figure 6 for Process 3. As a point of reference, the Figures include the results obtained from the empty H_{II} mesophase and published in ref 16.

As described in our previous work,[16] the structure of the water rods depends on the stability of the lipid−water interface, mainly consisting of GMO and its interaction, via H-bonding, with a layer of bound water. The PC, with its zwitterionic tail, is intercalated between them. TAG is intercalated between the hydrophobic tails.

CSA is a highly hydrophobic molecule, and originally, it was reasonable to assume that it was mainly incorporated between the acyl chains of the surfactants. However, FTIR studies[7] indicate that CSA is partially intercalated in the interfacial region via a partial replacement of the intramolecularly hydrogen-bonded carbonyl group bonds of the GMO headgroups to carbonyl−CSA bonds.

Process 1. Process 1 was identified with the rotation of the GMO headgroup.[16] These conclusions are confirmed by the CSA-induced change in the dielectric behavior of the GMO headgroups, evidenced in Process 1. This rotation necessitates the breaking of H-bonds between the β OH group (see the schematic in Figure 1) responsible for intramolecular binding. The critical temperature, $T_0 = 307$ K, noted in ref 16 as the temperature at which bound water disengages from the membrane interface, remains unchanged with the addition of CSA, as expected if the CSA molecule interacts with the GMO via carbonyl groups.

Furthermore, the dielectric strength of the process (Figure 3a) is lessened with the presence of CSA, an expected result if the headgroups face further restraint to orientation. Another conclusion of the FTIR study[5] was that the presence of the drug induces a slight dehydration of the GMO headgroup. Before the critical temperature, T_0, the dielectric strength demonstrates temperature behavior reminiscent of liquids, with deceasing dielectric strength as the temperature is increased. This indicates

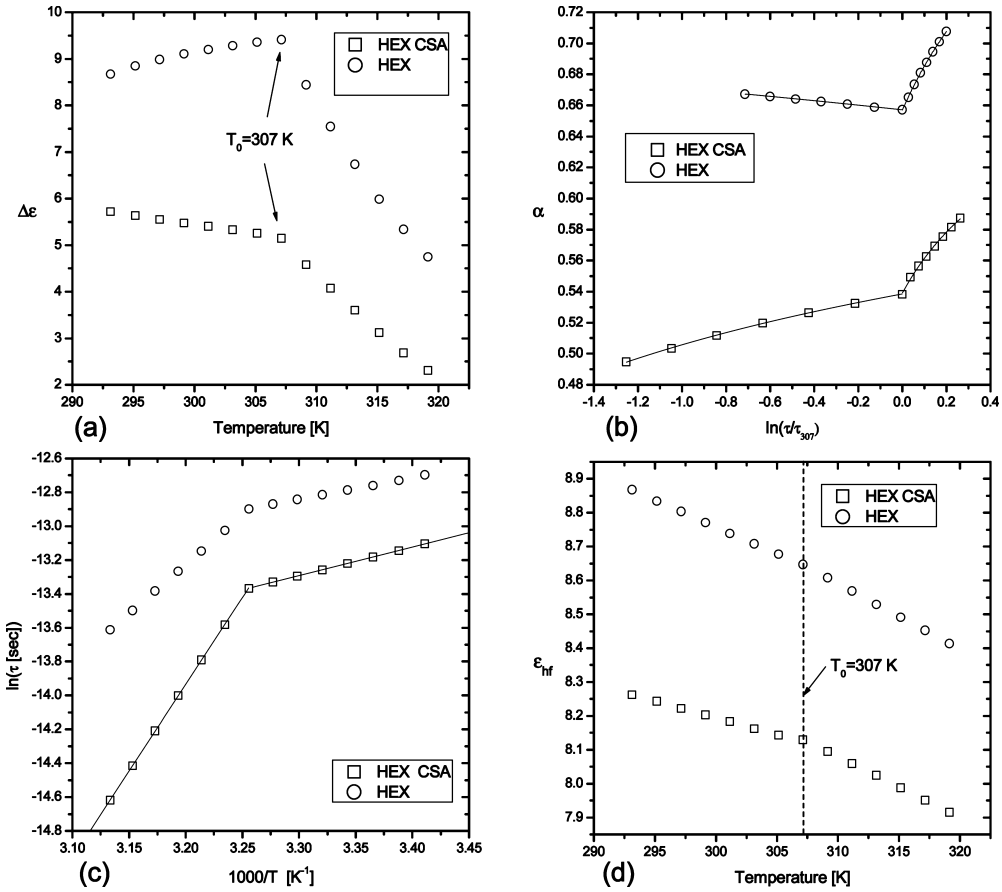

Figure 3. Fitting parameters (□) for Process 1 as a function of temperature: (a) The dielectric strength, $\Delta\varepsilon$, (b) the stretch parameter, α, as a function of the logarithm of the relaxation time (the relaxation times have been normalized by the relaxation time at $T = 307$ K, for clarity), (c) an Arrhenius plot of the relaxation times, τ, and (d) the high frequency limit of the dielectric permittivity, ε_{hf}. A comparison is made with the parameters for the empty system (○), reported in ref 15. The critical temperature $T_0 = 307$ K is evident throughout the data set in both samples.

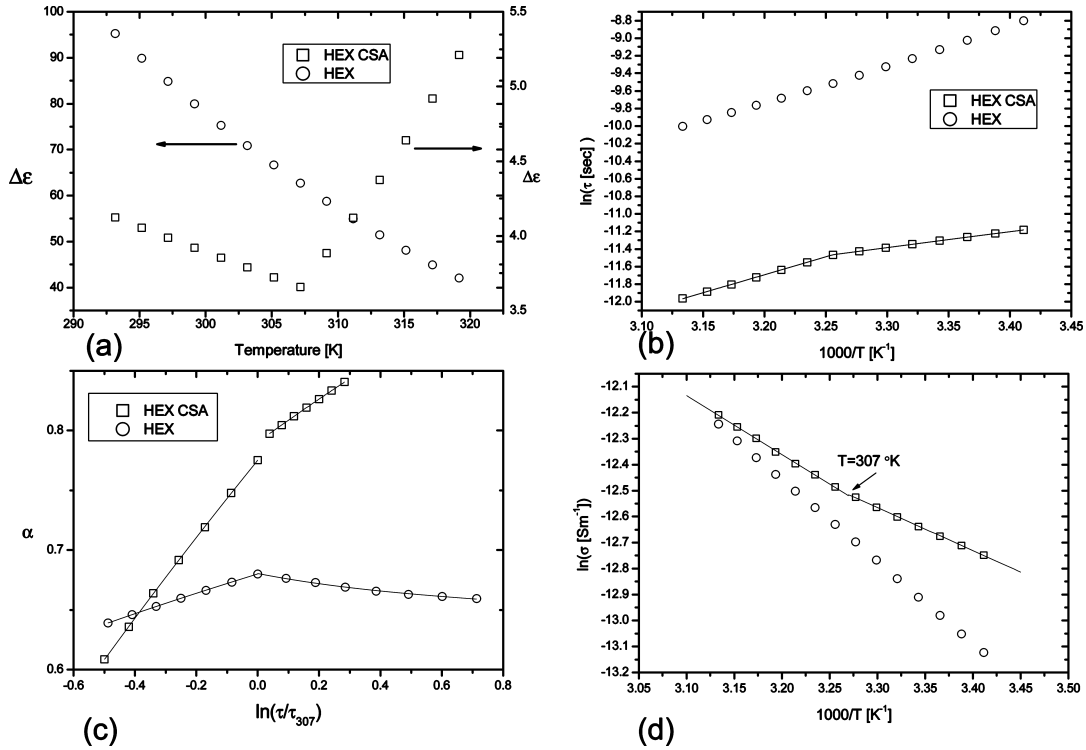

Figure 4. Fitting parameters of Process 2 and dc conductivity: (a) the dielectric strength, $\Delta\varepsilon$; (b) an Arrhenius plot of the relaxation times, τ; (c) the stretch parameter, α, as a function of the logarithm of the relaxation times, τ; and (d) the dc conductivity in an Arrhenius plot. For comparison, the results obtained for the empty H_{II} mesophase, reported in ref 1, are also plotted (○). In both samples the critical temperature, $T_0 = 307$ K is noted.

TABLE 1: Energies of Activation and Spatial Fractal Geometry for Processes 1 and 2 in the Presence of CSA and without it[a]

process		ΔE [kJ/mol]		d_g	
		$T < T_0$	$T > T_0$	$T < T_0$	$T > T_0$
Process 1	mpty	10.66	48.15	1.79	1.63
	with CSA	14.01	85.24	1.40	1.33
Process 2	empty	VFT behavior		2.59	1.26
	with CSA	15.14	33.9	3.66	7.10

[a] Values before and after the critical temperature, $T_0 = 307$ K, where the interface region of the GMO interface is de-hydrolyzed, are shown.

that the interfacial region is less stable in the presence of CSA. This stands in contrast with the situation without CSA.[16] The dehydration of the lipid layer after T_0 only serves to accentuate this trend. The present result is consistent with our previous rheological characterization of the system.[5] There it was revealed that solubilization of CSA had a destabilizing effect on the hexagonal phases. It caused a marked decrease in the elastic modulus of the systems and a progressive decrease in complex viscosity, leading to more liquid-like behavior and resulting in very short relaxation times (τ_{max} of 0.04 to 0.1 s). The decrease in τ_{max} and the elasticity of the systems were tentatively assigned to the intercalation of CSA to the interfacial region and its interaction with the carbonyl groups of the surfactants and weakening of the hydrogen bonds between the surfactant O−H groups and water.

More instructive is the Arrhenius plot of the relaxation times. The energies of activation derived from the Arrhenius plot of the relaxation times are also greater than those for the empty system. A comparison of their values for the empty system compared with those for the full system is presented in Table 1 for both Process 1 and Process 2. As before, in the temperature region below T_0, the energies of interaction are about half of the energy required to break a hydrogen bond, in line with one water molecule between two GMO headgroups. However, after T_0, when the interfacial layer dehydrates, the energy of activation for the CSA sample jumps to 85 kJ/mol, approximately four H-bonds. It was noted[6] when studying CSA in H_{II} mesophases that the peptide undergoes a conformational change, becoming more hydrophilic by partially disrupting the internal hydrogen bonds and exposing the amide groups to the surfactants. This "hydrophilization" of CSA comprises two internal H-bonds and amide groups and can account for the energy of activation noted above.

The behavior of the structural parameter, α, as a function of the logarithm of the relaxation times (Figure 3b) also demonstrates a dependence on the critical temperature, T_0. However, the fractal spatial dimension remains between 1 and 2, indicating that the relaxation occurs within the interboundary layer.

To summarize, the CSA molecule does not appear to interact with the interfacial water layer and only weakly affects the GMO head groups before the critical temperature, T_0. Above T_0, however, the competition between CSA and water for the intramolecular surfactant H-bonds is changed in favor of CSA as dehydration occurs. This leads to a conformal change in the CSA molecule, an effect already noted by Libster et al.,[5] increasing the energy of activation for the headgroup rotation of GMO.

Process 2. Process 2 was identified with counterion movement along the interface of the lipid layer.[16] In particular, the ionic headgroup of PC was shown to have a strong effect on this movement. With the presence of the CSA molecule in the interfacial region, it is to be expected that there will be further hindrance to counterion movement along the interfacial boundary and a strong influence will be introduced on the parameters of Process 2. The values of the fitting parameters $\Delta\varepsilon$, τ, and α as functions of temperature are presented in Figure 4. For the sake of clarity, the values obtained for the empty system are presented on the same graphs. Figure 4d is the dc conductivity.

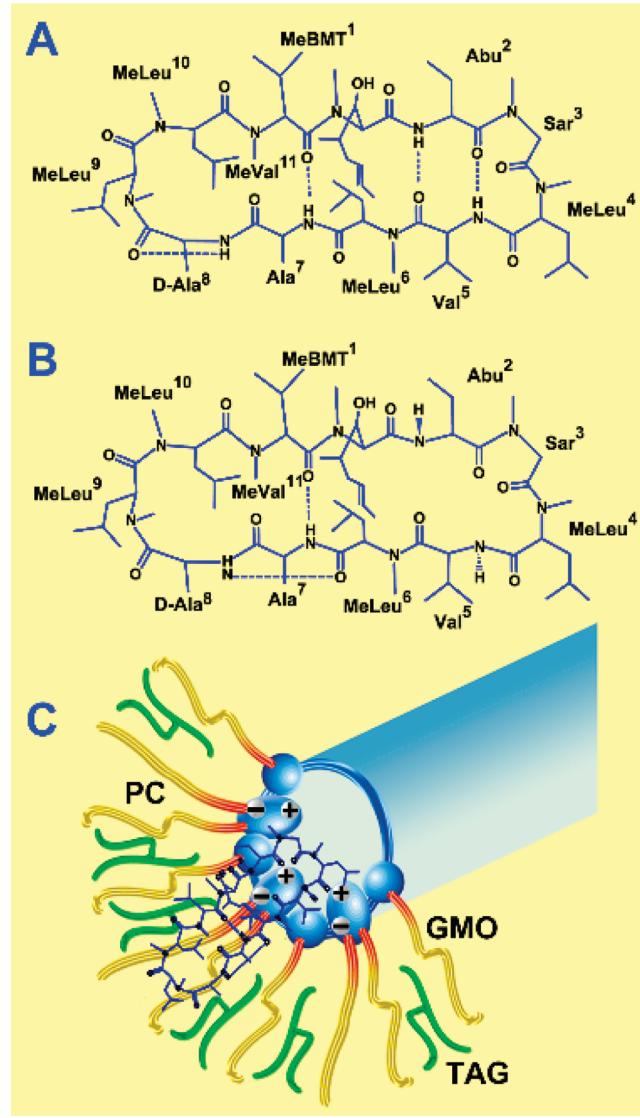

Figure 5. Conformations of CSA as explored by ATR-FTIR analysis in (A) tricaprylin, as control system (the structure of CSA is stabilized with four pairs of hydrogen bonds) and (B) in the H_{II} mesophase. Two pairs of hydrogen bonds, Abu^2NH to $Val^5C{=}O$ and Val^5NH to $Abu^2C{=}O$, were disrupted. (C) The peptide is partially intercalated into the interface region of the mesophase as a result of the disruption of two pairs of internal hydrogen bonds that are available to interact with water or the surfactant heads.

In fact, the relaxation times do demonstrate a dramatic departure from their behavior in the empty system. Previously, it had been noted that the thermal behavior of the relaxation times in the empty system exhibited Vogel−Fulcher−Tammenn (VFT)[17,21] temperature dependence (i.e., $\ln(\tau) = \ln(\tau_0) + (FT_x)/((T - T_x))$, where T_x is a critical temperature and F is known as the fragility of the process). This was significant because VFT behavior is indicative of a cooperative relaxation, not something to be expected in counterion movement. It was shown[16] that if the motion was retarded by the PC headgroup then it would be influenced by weak cooperativity between the zwitterionic tails of the PC. Consequently, the same cooperativity would be manifested in the thermal behavior of the counterion relaxation

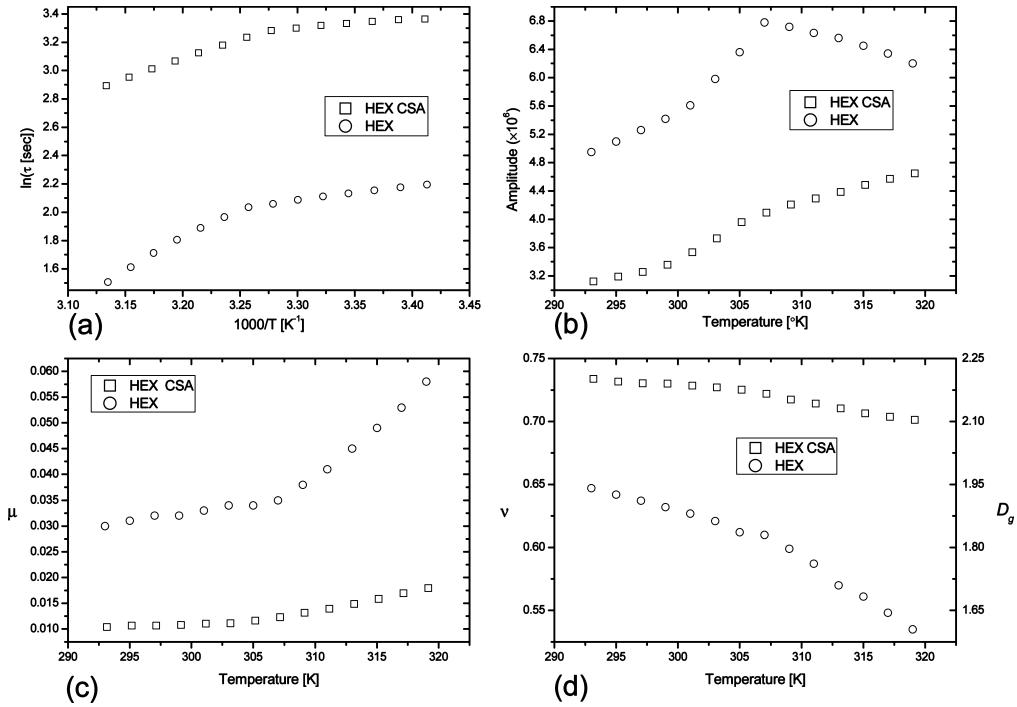

Figure 6. Fitting parameters of Process 3: (a) the relaxation times on an Arrhenius plot, (b) the amplitude of the process as a function of temperature, (c) the power parameter of eq 4, and (d) the stretch parameter of eq 4. The data for the empty H_{II} system are taken from Ishai et al.[15]

times. With the presence of CSA, all cooperative motion is lost. Instead, typical Arrhenius behavior is retained with differing energies of interaction before and after T_0. These are summarized in Table 1. For temperatures less than T_0, the energy of activation is 15 kJ/mol, in line with typical energies of activation for counterion hopping. However, above T_0, the energy increases significantly ($\Delta E = 33.9$ kJ/mol). Whereas it is still low in terms of the energies of trapped counterions (~60 kJ/mol),[28] it points to a greatly retarded motion, a quasi-trap. The loss of cooperative motion in the presence of CSA is supported by our previous findings, performed by ATR-FTIR measurements, relating to molecular interactions of CSA with the mesophase components.[7] On the molecular level, a dehydration of the GMO hydroxyls is a result of CSA incorporation, suggesting a weak interaction of the peptide with the O−H groups in the interfacial water region. The observed interfacial interactions of CSA within the mesophases were enabled by specific conformational changes of this peptide when two pairs of its internal hydrogen bonds were disrupted. As a result of this, the original structure of the cyclic peptide was destabilized, probably rearranging into a more open conformation that interacts with the polar or amphiphilic parts of the host structure. The partial disruption of the internal hydrogen bonds of the CSA frame caused a rotation of the involved peptide amide groups outward, resulting in more efficient intermolecular hydrogen bonds. (See Figure 5.) Apparently, the same peptide functional groups, which were free to participate in bonding with the aqueous phase, are responsible for strong interactions with counterions. Such interactions were reflected in atypically high activation energies for ion hopping. On the whole, it is known that extremely high activation energies are characteristic for ions entrapped within biomacromolecular structures. For example, the energy of activation of two alkali metal ion (Na^+ and K^+) complexes with an enzyme (pyruvate kinase), entrapped in the low water environment of reverse micelles, was found to be in the range of 280−415 kJ/mol.[29] Certainly, the large dimensions of pyruvate kinase cannot be directly compared with CSA peptide, but high activation energies due to a complex formation are valid in both cases.

More intriguing is the fractal spatial dimension for the process. As can be seen from Table 1 the values are greater than 3. The motion of the counterion through the interfacial layer is necessarily diffusive in nature. In essence, the measurement is one of a virtual dipole. As such, there are a number of different length scales to consider, depending on the various types of interaction of the ion with the interface: (1) between GMO headgroups through the H-bond network, (2) between the PC ion headgroups and the relatively long time scale static interaction, and (3) in the region of the CSA intrusion to the interface. Fractal dimensions greater than 3 (see Table 1) would imply anomalous diffusion of the counterion, whereby long-range super diffusive behavior[30] would be evident. This would point to CSA concentrating many carriers in its vicinity, providing the conditions for a complicated fractal structure.

Finally, the dielectric strength of the process when $T < T_0$ demonstrates liquid-like behavior with $\Delta\varepsilon$ decreasing as the temperature is increased. Above T_0, there is a dramatic increase in dielectric strength as the loosening of the interface increases the influence of CSA. The increase in $\Delta\varepsilon$ indicates either an increase in the number of charge carriers or a strengthening of the virtual dipoles they create. Because this virtual dipole moment is proportional to the mean free path, the charge will move in the time window of measurement, leading one to conclude that superdiffusive motion is prevalent, in collusion with the derived fractal dimension.

The modification of the relaxation behavior of counterions in H_{II} mesophases, induced by the presence of CSA, confirms the results of Libster et al.[6] Namely, the fact that the CSA is intercalated between the tails of the surfactant but significantly intrudes into the interface. The dehydration of the surfactant heads leads to a stronger interaction of the CSA molecule with them and, consequently, a conformal change in the peptide. This, in turn, influences counterion movement, leading to anomalous diffusion of these elements.

Process 3. Process 3 was previously identified with the percolative motion of tricaprylin through the surfactant tails.[16]

Usually, the temperature dependence of parameters μ and ν reflects the approach of the system to a percolative state, whereby an "infinite" cluster exists at the percolation threshold through which the dipole motion can occur.[17,27] The power law dependence of eq 4 dominates on the long time scales, whereas short times are ruled by the stretched exponent. Physically speaking, mesoscalar relaxations of the cluster are the accumulations of fast microscopic movements inside the cluster. This point is emphasized in the derivation of eq 4 based on the static site lattice model.[17] The distribution of cluster sizes over the lattice is given by

$$W(s, s_m) = C_m s^{-\Omega} \exp(^{-s}/_{s_m}) \quad (5)$$

where s is the cluster size, s_m is the maximum cluster size, and C_m is normalization constant. The exponent Ω is a scaling coefficient of the probability "per lattice site" that the site belongs to the s cluster, known as the polydispersity index. It can be related to the coefficients of the power and stretch expression of eq 4 by the relationship[27]

$$\Omega = \frac{\mu}{\nu} + \frac{1}{2} \quad (6)$$

It was also shown by Maurin et al.[28] that the spatial fractal dimension through which the transport occurs is given by $d_g = 3\nu$. Combining this with expression 6, one can interpret to be a measure of the diversity of available volume relaxations. Succinctly put, the lower the value of μ, the more homogeneous the distribution of cluster sizes contributing to a relaxation. In this model, the transition of the system from an unpercolated state to a percolated state is accompanied by a monotonic rise in the value of ν and a monotonic decrease in the value of μ as the temperature increases. Immediately above the percolation temperature threshold, these tendencies are reversed.[27] Consequently, model parameters in Figure 6c,d are reminiscent of a system already percolated. The temperature dependence of μ (Figure 6c) with and without CSA shows that as temperatures are raised there is a general loosening of the tail network through which the TAG molecules move but that the cluster network in the CSA system is more homogeneous. The critical temperature $T_0 = 307$ K is strongly evident in the empty system but in the CSA loaded system is not overtly noticeable. Consequently, the presence of CSA also stabilizes the hydrophobic tail region of the gel. The static fractal dimension of the gel, evidenced through the ν temperature dependence, is ~2.1, demonstrating that the TAG is mainly moving along the road surface. The relaxation times are also longer than those in the empty system, an expected consequence of the stiffened environment due to the presence of CSA.

Conclusions

The effect of CSA on the dielectric behavior of H_{II} mesophases was investigated. In concurrence with previous works in FTIR, the changes in response wrought by the presence of the CSA molecule point to its partial intercalation into the H_{II} interface. This was particularly clear when considering its influence on counterion motion along the interface between the lipid headgroups and the bound water layer, as evidenced in Process 2. Whereas the critical temperature for dehydration of the lipid layer remained unaffected, the energy of activation of the process demonstrates that the motif of movement becomes one of trapping once dehydration has occurred. Furthermore, the fractal dimension in which this relaxation can occur becomes superdiffusive. The rotation of the GMO headgroup, evidenced by Process 1, also demonstrated the influence of CSA. Before the dehydration point, the energy of activation of the empty system and the CSA-loaded system are similar, reinforcing the view that the interaction of the CSA molecule with GMO is mainly via the carbonyl groups in the tails. However, above T_0, the energies jump as the OH^- groups begin to interact with exposed OH^- groups on the CSA molecule as well. Finally, the motion of tricaprylin along the outside of the water rods shows that the CSA molecule does in fact stabilize this region as well, leading to a stiffening of the hydrophobic compartments of the gel.

References and Notes

(1) Boyd, B. J.; Whittaker, D. V.; Khoo, S.; Davey, G. *Int. J. Pharm.* **2006**, *318*, 154–162.
(2) Boyd, B. J.; Khoo, S.; Whittaker, D. V.; Davey, G.; Porter, C. J. *Int. J. Pharm.* **2007**, *340*, 52–60.
(3) Lopes, L. B.; Speretta, F. F.; Bentley, M. V. L. *Eur. J. Pharm. Sci.* **2007**, *32*, 209–215.
(4) Lynch, M. L.; Ofori-Boateng, A.; Hippe, A.; Kochvar, K.; Spicer, P. T. *J. Colloid Interface Sci.* **2003**, *260*, 404–413.
(5) Libster, D.; Aserin, A.; Wachtel, E.; Shoham, G.; Garti, N. *J. Colloid Interface Sci.* **2007**, *308*, 514–524.
(6) Libster, D.; Ishai, P. B.; Aserin, A.; Shoham, G.; Garti, N. *Int. J. Pharm.* **2009**, *367*, 115–126.
(7) Libster, D.; Aserin, A.; Yariv, D.; Shoham, G.; Garti, N. *J. Phys. Chem. B* **2009**, *113*, 6336–6346.
(8) Italia, J.; Bhardwaj, V.; Ravi Kumar, M. *Drug Discovery Today* **2006**, *11*, 846–854.
(9) Lopes, L.; Ferreira, D.; De Paula, D.; Garcia, M.; Thomazini, J.; Fantini, M.; Bentley, M. *Pharm. Res.* **2006**, *23*, 1332–1342.
(10) Lambros, M.; Rahman, Y. *Chem. Phys. Lipids* **2004**, *131*, 63–69.
(11) Libster, D.; Ben Ishai, P.; Aserin, A.; Shoham, G.; Garti, N. *Langmuir* **2008**, *24*, 2118–2127.
(12) Amar-Yuli, I.; Wachtel, E.; Ben Shoshan, E.; Danino, D.; Aserin, A.; Garti, N. *Langmuir* **2007**, *23*, 3637–3645.
(13) Amar-Yuli, I.; Wachtel, E.; Shalev, D.; Moshe, H.; Aserin, A.; Garti, N. *J. Phys. Chem. B* **2007**, *111*, 13544–13553.
(14) Amar-Yuli, I.; Wachtel, E.; Shalev, D.; Aserin, A.; Garti, N. *J. Phys. Chem. B* **2008**, *112*, 3971–3982.
(15) Bonacucina, G.; Palmieri, G. F.; Craig, D. Q. *J. Pharm. Sci.* **2005**, *94*, 2452–2462.
(16) Ben Ishai, P.; Libster, D.; Aserin, A.; Garti, N.; Feldman, Y. *J. Phys. Chem. B* **2009**, *113*, 12639–12647.
(17) Feldman, Y.; Puzenko, A.; Ryabov, Y. In *Advances in Chemical Physics, Part A, Fractals, Diffusion and Relaxation in Disordered Complex Systems*; John Wiley & Sons: New York, 2006; Vol. 133, pp 1−125.
(18) *"Alpha High Resolution Dielectric Analyser"* User's Manual; Novocontrol GmbH: Hamburg, 2000.
(19) Axelrod, N.; Axelrod, E.; Gutina, A.; Puzenko, A.; Ben Ishai, P.; Feldman, Y. *Meas. Sci. Technol.* **2004**, *15*, 755–764.
(20) *Matlab*; MathWorks. Mathworks Inc: Natick, MA, 2009.
(21) Kremer, F.; Schönhals, A. *Broadband Dielectric Spectroscopy*, 1st ed.; Springer: New York, 2002.
(22) Cole, K. S.; Cole, R. H. *J. Chem. Phys.* **1941**, *9*, 341–351.
(23) Davidson, D.; Cole, R. H. *J. Chem. Phys.* **1951**, *19*, 1484–1490.
(24) Ryabov, Y. E.; Feldman, Y. *Physica A* **2002**, *314*, 370–378.
(25) Ben Ishai, P. *Dielectric Relaxation in KTN Ferroelectric Crystals as a Result of Dopants*. Ph.D. Dissertation, The Hebrew University of Jerusalem: Jerusalem, 2009.
(26) Metzler, R.; Klafter, J.; Sokolov, I. *Phys. Rev. E* **1998**, *58*, 1621–1633.
(27) Feldman, Y.; Puzenko, A.; Ryabov, Y. *Chem. Phys.* **2002**, *284*, 139–168.
(28) Maurin, G.; Devautour, S.; Henn, F.; Giuntini, J.; Senet, P. *J. Chem. Phys.* **2002**, *117*, 1405–1408.
(29) Saavedra-Lira, E.; Ramirez-Silva, L.; Perez-Montfort, R. *FASEB J.* **1997**, *11*, A1437–A1437.
(30) Metzler, R.; Barkai, E.; Klafter, J. *Phys. Rev. Lett.* **1999**, *82*, 3563–3567.

JP104028M